CHEMISTRY
AN ASIAN JOURNAL

DOI: 10.1002/asia.200700163

Tunable Bacterial Agglutination and Motility Inhibition by Self-Assembled Glyco-Nanoribbons

Yong-beom Lim,[a] Somi Park,[a] Eunji Lee,[a] Ja-Hyoung Ryu,[a] You-Rim Yoon,[a] Tae-Hyun Kim,[b] and Myongsoo Lee*[a]

Abstract: We explored a method of controlling bacterial motility and agglutination by using self-assembled carbohydrate-coated β-sheet nanoribbons. To this aim, we synthesized triblock peptides that consist of a carbohydrate, a polyethylene glycol (PEG) spacer, and a β-sheet-forming peptide. An investigation into the effect of PEG-spacer length on the self-assembly of the triblock peptides showed that the PEG should be of sufficiently length to stabilize the β-sheet nanoribbon structure. It was found that the stabilization of the nanoribbon led to stronger activity in bacterial motility inhibition and agglutination, thus suggesting that antibacterial activity can be controlled by the stabilization strategy. Furthermore, another level of control over bacterial motility and agglutination was attained by co-assembly of bacteria-specific and -nonspecific supramolecular building blocks. The nanoribbon specifically detected bacteria after the encapsulation of a fluorescent probe. Moreover, the detection sensitivity was enhanced by the formation of bacterial clusters. All these results suggest that the carbohydrate-coated β-sheet nanoribbons can be developed as promising agents for pathogen capture, inactivation, and detection, and that the activity can be controlled at will.

Keywords: carbohydrates · cell recognition · nanostructures · peptides · self-assembly

Introduction

The process of molecular self-assembly is mediated by iterative noncovalent interactions among monomeric building blocks,[1] which makes self-assembled nanostructures excellent platforms for attaching multiple functional moieties.[2] As carbohydrates are structurally diverse and a myriad of biological recognition events are mediated by carbohydrate–carbohydrate or carbohydrate–protein interactions, the attachment of carbohydrates on self-assembled nanostructures offers a unique opportunity to modulate many carbohydrate-dependent biological processes.[2,3a–d] In multivalent-type interactions, the binding constant is significantly larger than the simple arithmetic sum of the respective monovalent interactions.[3] For this reason, carbohydrate-attached multivalent molecules and nanostructures have been utilized as competitive inhibitors of carbohydrate-dependent pathogen–cell interactions, bacterial-toxin–cell interactions, and cancer metastasis.[4] Furthermore, they have also been used as cross-linkers for cell aggregation.

The agglutination and motility inhibition of pathogenic cells such as bacteria, virus, and spores by carbohydrate-attached multivalent nanostructures was recently investigated for potential applications in pathogen capture, inactivation, and detection.[5] Examples include carbohydrate-functionalized carbon nanotubes (CNTs), gold nanoparticles, polyglycine nanosheets, rod–coil amphiphiles, and β-sheet peptide nanoribbons. It was shown that fiberlike nanostructures such as CNTs and β-sheet peptide nanoribbons are especially suitable for aggregating cells, thus indicating that nanostructures of sufficient length are necessary for cross-linking cells.

The design principle of most artificially designed β-sheet peptides is the alternating placement of positively charged, hydrophobic and negatively charged amino acids.[5a,6] Attraction between oppositely charged amino acids and solvopho-

[a] Dr. Y.-b. Lim, S. Park, E. Lee, Dr. J.-H. Ryu, Y.-R. Yoon, Prof. Dr. M. Lee
Center for Supramolecular Nano-Assembly
Department of Chemistry
Yonsei University
Seoul 120-749 (Korea)
Fax: (+82) 2-393-6096
E-mail: mslee@yonsei.ac.kr

[b] Prof. Dr. T.-H. Kim
Department of Chemistry
University of Incheon
Incheon 402-749 (Korea)

Supporting information for this article is available on the WWW under http://www.chemasianj.org or from the author.

bic interactions between hydrophobic amino acids are the primary driving forces for the proper β-sheet hydrogen-bonding arrangement. Iterative edge-to-edge and face-to-face β-sheet packing of β-sheet peptides lead to the formation of a nanoribbon structure. The β-sheet peptide nanoribbons are excellent scaffolds for functionalization with bioactive molecules such as carbohydrates, peptides, and proteins.[5a,6a–c] Mannose-coated β-sheet nanoribbons were shown to agglutinate and/or inhibit bacterial motility by specific multivalent interactions of the mannose residues with mannose-binding proteins (MBPs) in the pili of *Escherichia coli*.[5a]

It has been demonstrated that peptides with a propensity for β-sheet formation self-assemble into a hierarchy of nanostructures in solution, such as tapes, ribbons, fibrils, and fibers.[7] The fibrils and fibers are lateral aggregates of the β-sheet tapes and ribbons. The coupling of hydrophilic macromolecules on the N or C terminus of β-sheet peptides has a significant influence on the self-assembly process of block peptides. It was reported that coupling of polyethylene glycol (PEG) on β-sheet peptides can suppress the lateral aggregation of β-sheet nanostructures and enhance their solubility in aqueous solution.[8] Furthermore, it was found that the morphologies of the β-sheet nanostructures formed are influenced by the structure of the PEG blocks. Bulky and dendritic PEG structures interfere with the formation of a proper β-sheet arrangement of the block β-sheet peptide, thus resulting in premature termination of nanoribbon growth.[5a] Accordingly, nanoribbons from a peptide with a bulky and dendritic PEG block was found to be significantly shorter than those formed from one with a linear PEG block. These previous findings suggest that the properties of the hydrophilic segment have a significant influence on the supramolecular structure of β-sheet peptide block molecules. Moreover, the biological activity of differently sized nanoribbons in terms of bacterial agglutination and motility inhibition was found to be significantly different.

However, it has not been established how the PEG block length affects the self-assembly characteristics of β-sheet peptides. Herein, we report a strategy to control the degree of *E. coli* agglutination and motility by carbohydrate-functionalized β-sheet peptide nanoribbons. To this aim, we first investigated how the PEG block length affects the stability and length of the nanoribbons formed from a carbohydrate, a PEG spacer, and a β-sheet peptide triblock molecule. Second, we investigated how the supramolecular stability and length of the carbohydrate-coated nanoribbons are related to *E. coli* binding activity. We then developed a way to fine-tune *E. coli* binding activity further by co-assembling the triblock peptides that contain an MBP-specific and a nonspecific carbohydrate. Finally, the possibility of specifically detecting bacteria was investigated with this carbohydrate-coated nanoribbon upon encapsulation of a fluorescent dye. This study should be a critical step toward the development of better pathogen-capture, inactivation, and detection agents.

Abstract in Korean:

자기 조립되어 탄수화물로 촘촘히 둘러 싸인 베타쉿 나노리본을 이용하여 박테리아의 유동성을 저해시키고 응집시키는 방법을 연구하였다. 이 실험을 위해서 탄수화물, 연결부위, 그리고 베타쉿을 형성하는 펩타이드로 이루어진 초분자 단위체를 만들었다. 실험결과 연결부위의 길이가 어느 정도 충분이 길어야 베타쉿 나노리본 구조가 안정화 된다는 것을 밝혀내었다. 그리고 나노리본의 안정화와 박테리아 유동성 저해/응집에는 상관관계가 있음을 알게 되었다. 이것은 안정화 전략에 의하여 나노리본의 항균성을 마음대로 조절할 수 있다는 것을 보여준다. 또한 박테리아에 선택적으로 결합하는 탄수화물과 그렇지 않은 탄수화물로 이루어진 초분자 단위체를 공자기조립 시키는 방법으로 나노리본의 항균성이 더 미세하게 조절될 수 있다는 것을 보여주었다. 나노리본은 형광을 띠는 소수성 분자를 함유하는 성질을 띠었고, 이렇게 형광물질이 함유된 나노리본은 특정 탄수화물에 결합하는 박테리아를 선택적으로 검출할 수 있었다. 위 결과들은 탄수화물로 둘러 싸인 베타쉿 나노리본이 병원균을 포획, 응집, 그리고 검출하는 물질로 이용, 개발 될 수 있다는 가능성을 제시하고 있으며, 그 활성도를 원하는 대로 조절할 수 있는 방법을 개발하였다는 것을 보여준다.

Results and Discussion

Carbohydrate-Coated Self-Assembling Peptides

The triblock molecules that consist of a carbohydrate, a PEG, and a β-sheet peptide were synthesized by using solid-phase organic/peptide-synthesis methods similar to those[5a] described previously (Scheme 1). The β-sheet peptide block (FKFEFKFEF) was synthesized by using standard Fmoc (9-fluorenylmethoxycarbonyl) chemistry on Rink amide MBHA (4-methylbenzhydrylamine) resin. The sequence of the peptide has been shown to form β-sheet nanoribbons in

CHEMISTRY
AN ASIAN JOURNAL

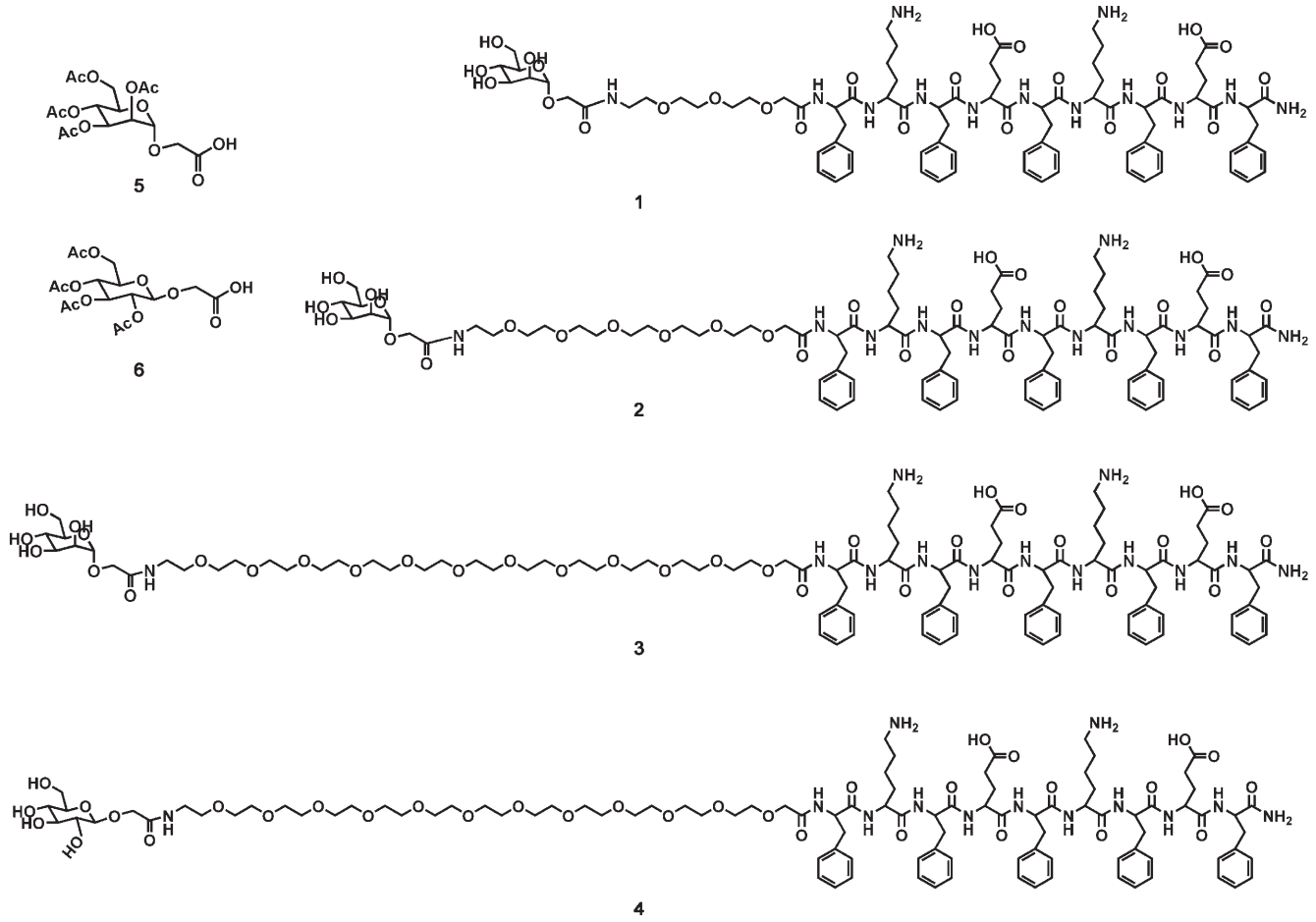

Scheme 1. Structures of carbohydrate-coated nanoribbon building blocks. **1** ($n=3$), **2** ($n=6$), and **3** ($n=12$): Mannose building blocks. **4** ($n=12$): A glucose building block. **5** = carboxymethyl 2,3,4,6-tetra-*O*-acetyl-α-D-mannopyranoside, **6** = carboxymethyl 2,3,4,6-tetra-*O*-acetyl-β-D-glucopyranoside.

aqueous solution. Coupling of the Fmoc-NH-$(EG)_n$-COOH (EG = ethylene glycol, n = degree of polymerization = 3, 6, or 12) section of different ethylene glycol units was achieved by HBTU (2-(1*H*-benzotriazol-1-yl)-1,1,3,3-tetramethyluronium hexafluorophosphate)-mediated activation of the carboxy group. After removal of the Fmoc group from the PEG, **5** was coupled and its acetyl groups removed by 10% hydrazine in DMF (*N*,*N*-dimethylformamide) to make an α-D-mannose-functionalized nanoribbon building block. A β-D-glucose-functionalized building block was synthesized similarly by using **6**. Cleavage and side-chain deprotection by TFA (trifluoroacetic acid) yielded the triblock molecules **1**–**4**. The triblock molecules were purified by reverse-phase (RP) HPLC (>95% purity), and the molecular weight was confirmed by MALDI-TOF mass spectrometry.

The self-assembly of the block molecules was investigated by circular dichroism (CD) spectroscopy, which showed that all the molecules formed β sheets, as evidenced by the minima in molar ellipticity at 215 nm (Figure 1a). Transmission electron microscopy (TEM) of the nanostructures revealed the formation of nanoribbons[5a] (Figure 1b). As shown in Figure 1a, the molar ellipticity at 215 nm became stronger as the PEG chain length increased, which is an indication of a stronger association of β strands. It was reported that the degree of association correlates with the stabilization of the β-sheet structure, which in turn produces longer assemblies.[6a,9] Therefore, the results suggest that the PEG should be of sufficient length to stabilize the β-sheet nanostructure, and that the supramolecular length of the nanoribbons increases with PEG chain length. It was reported that β-sheet nanostructures can be stabilized by adding more β-sheet-forming sequences in the peptide.[9] β-Sheet stabilization in this type of block-peptide system should be affected by contributions from both the hydrophilic and the β-sheet-forming blocks. On the basis of this new finding that a hydrophilic block of a certain length helps to stabilize β-sheet interaction, it would be interesting to find the maximum length of hydrophilic block that a β-sheet peptide block can tolerate, above which β-sheet interaction might be weakened due to steric hindrance; this point could be the subject of further study.

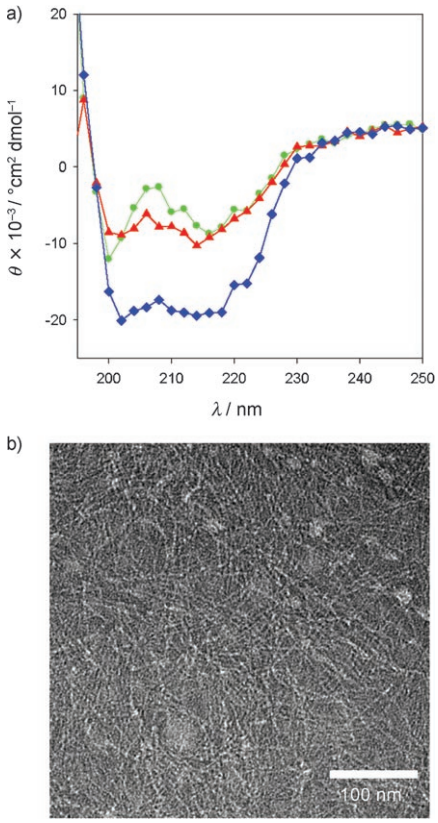

Figure 1. Self-assembly of triblock peptides. a) CD spectra of **1** (green), **2** (red), and **3** (blue). b) Negatively stained TEM image of **3**. TEM images of **1**, **2**, and **4** are similar (data not shown).

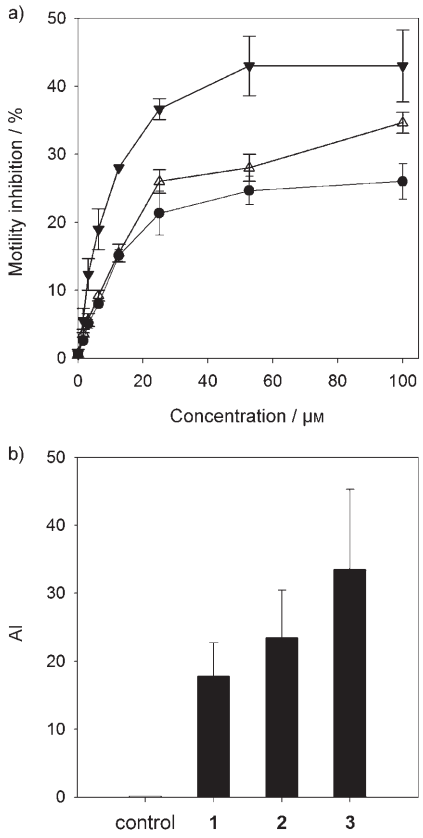

Figure 2. The effect of stabilization of the mannose-coated nanoribbons and formation of longer assemblies on motility inhibition and agglutination of *E. coli* ORN178. a) Bacterial motility-inhibition assay. ● = **1**, △ = **2**, ▼ = **3**. Each data point represents the mean ± SD (standard deviation; $n = 5$). b) Bacterial agglutination assay. The concentration was 50 μM. Control: monovalent mannose (α-methyl-D-mannopyranoside). Each bar represents the mean ± SD ($n = 10$). AI = agglutination index.

Control of *E. coli* Mobility and Agglutination

The *E. coli* strain ORN178 expresses mannose-binding adhesin FimH in its type 1 pili.[10] The type 1 pili are filamentous appendages produced by many members of gram-negative bacteria. It was reported that multivalent binding of mannose residues in nanostructures with FimH in *E. coli* ORN178 leads to the agglutination and/or motility inhibition of the bacteria.[5a,b]

To examine the effect of β-sheet stabilization on *E. coli* binding activity of the nanoribbons, *E. coli* ORN178 motility-inhibition and agglutination assays[5a,b] were performed. As shown in Figure 2a, the bacteria gradually lost their motility when treated with increasing concentrations of mannose-coated nanoribbons. However, the increase in ability to inhibit bacterial motility had a positive correlation with nanoribbon stabilization and the formation of longer assemblies. With regard to bacterial agglutination, the nanoribbons from **1**, **2**, and **3** could agglutinate treated bacteria, which indicates that all the nanoribbons are long enough to cross-link the bacteria[5a] (Figures 2b and 4). However, a clear difference was also observed among the nanoribbons in their ability to agglutinate the bacteria. The more stable and longer nanoribbons agglutinated the bacteria better.

These results indicate that there is a strong correlation between bacterial motility inhibition/agglutination and nanoribbon stabilization/formation of longer assemblies. Another possibility is that longer PEG chains may enable a more precise arrangement of the mannose residue on the FimH protein owing to the enhanced degrees of freedom relative to the conformationally more rigid and shorter PEG chains.[3a]

Notably, *E. coli* strain ORN208, a FimH gene mutant in which the mannose-binding ability of FimH has been inactivated, neither lost its motility nor was agglutinated by the addition of any nanoribbons. Furthermore, both motility-inhibited and agglutinated *E. coli* ORN178 returned to their original mobile and dispersed state when a specific competitor, α-methyl-D-mannopyranoside, was added in large excess (1000×), thus indicating the reversible nature of the phenomenon. By contrast, a nonspecific competitor, D-(+)-galactose, had no influence on the motility-inhibited and agglutinated bacteria. All this evidence indicates that the interactions are specific.

Next, we asked whether we could have another level of control over bacterial motility and agglutination with the carbohydrate-coated nanoribbons. For this, we co-assembled the mannose building block **3** with the glucose building

block **4**.[6b] FimH protein is specific only to mannose residue. As shown in Figure 3, bacterial motility and AI decreased as the relative proportion of the glucose building block incorporated in the nanoribbons increased. By increasing the proportion of the glucose building block from 0 to 100%, bacterial motility and AI decreased by a factor of 24 and 7, respectively. These results indicate that bacterial motility and AI can be controlled in predictable and tunable ways by changing the composition of specific and nonspecific nanoribbon building blocks.

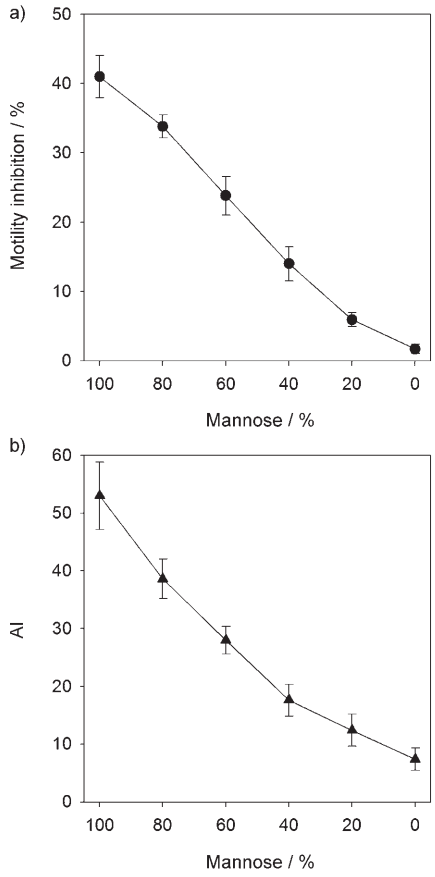

Figure 3. Fine-tuning of bacterial motility and agglutination by molecular co-assembly of specific and nonspecific building blocks. a) Bacterial motility-inhibition assay. Each data point represents the mean ± SD ($n=5$). b) Bacterial agglutination assay. Each data point represents the mean ± SD ($n=10$). The relative proportion of glucose building blocks changed from 0 to 100%. The total concentration of the building blocks was 50 μM.

Carbohydrate-Coated Nanoribbons for Specific Detection of Pathogens

The development of fast and reliable methods for detecting pathogens is in high demand for clinical and food-testing uses.[11] As the β-sheet nanoribbon structure can encapsulate hydrophobic compounds between the hydrophobic interface formed by the bilayer of β tapes,[6a] we next asked whether carbohydrate-coated nanoribbons can be used for the specific detection of pathogens following encapsulation of the hydrophobic fluorescent probe. *E. coli* ORN178 is a good model pathogen as FimH in the type 1 pili is encoded by most strains of uropathogenic *E. coli*. FimH binds to mannosylated host receptors present on the epithelium of the bladder, thus causing urinary-tract infections.[12]

Following encapsulation of the hydrophobic fluorescent probe nile red in the nanoribbons of **3**, *E. coli* ORN178 was induced to form clusters (Figure 4). The bright-field image reveals the agglutination of the bacteria (Figure 4a). The

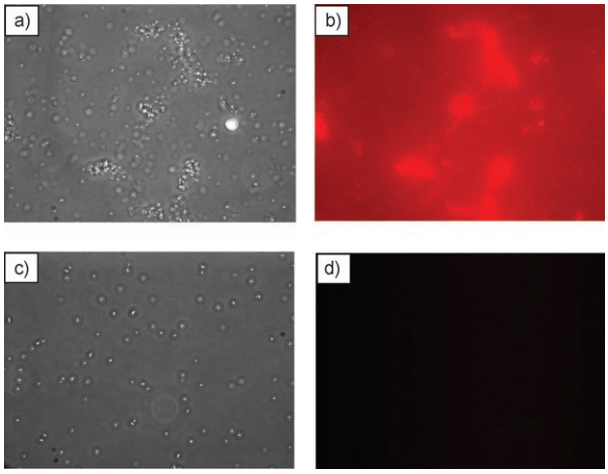

Figure 4. Potential application of fluorescent-probe-encapsulated carbohydrate-coated nanoribbons for detection of pathogenic bacteria. a) Phase-contrast bright-field image of *E. coli* ORN178 agglutinated by the treatment of nile red encapsulated **3**. b) Nile red fluorescence image of the specimen in a). c) Phase-contrast bright-field image of *E. coli* ORN208 treated with nile red encapsulated **3**. d) Nile red fluorescence image of the specimen in c). The concentration of **3** was 50 μM, and 2 mol% of nile red relative to **3** was encapsulated. Magnification: 400×.

fluorescence image of the same field clearly shows bright-red fluorescence from bacterial clusters (Figure 4b). The bacteria not incorporated in the bacterial cluster also fluoresce, but fluorescence from the cluster is far brighter. The results imply that sensitivity in bacterial detection can be enhanced by cluster formation. Therefore, the fact that triblock peptides can form long nanostructures that agglutinate bacterial cells is an added benefit for making a highly sensitive method of bacterial detection. The *E. coli* ORN208 strain was neither agglutinated nor detected with the nile red encapsulated nanoribbon, thus showing the specificity of the detection (Figure 4c and d).

Conclusions

We have shown that the degree of bacterial motility and agglutination can be controlled by stabilization and variation in the length of carbohydrate-coated β-sheet nanoribbons. Furthermore, another level of fine-tuning in antibacterial activity was possible by co-assembling *E. coli* specific and nonspecific supramolecular building blocks. The carbohydrate-coated β-sheet nanoribbons not only detected bacteria spe-

cifically following encapsulation of fluorescent probes, but the sensitivity was also enhanced owing to bacterial clustering. These results indicate that this type of carbohydrate-coated β-sheet nanoribbon can be developed as promising agents for pathogen capture, clearance, and detection, and that we can finely control the antibacterial activity at will.

Experimental Section

Synthesis of Triblock Peptides

The β-sheet-peptide portion of the triblock peptides (FKFEFKFEF) was synthesized on Rink amide MBHA resin (Anaspec, USA) by using standard Fmoc protocols on an Applied Biosystems model 433A peptide synthesizer. Fmoc-NH-$(EG)_n$-COOH was synthesized as described previously[5a] and was further purified by preparative recycling gel-permeation chromatography (GPC) (polydispersity index <1.1). Fmoc-NH-$(EG)_n$-COOH ($n=3$, 6, and 12) was coupled to the peptide on the resin in a 6-mL polypropylene tube with frits (Restek, USA). The peptide-attached resin (100 mg, 35 μmol of N-terminal amine groups, substitution on the resin: 0.35 mmol g^{-1}) was swollen in *N*-methyl-2-pyrrolidone (NMP) for 30 min. Before addition to the resin, the mixture of Fmoc-NH-$(EG)_n$-COOH (175 μmol), HBTU (61 mg, 160 μmol), HOBt (1-hydroxybenzotriazole; 22 mg, 160 μmol), and DIPEA (diisopropylethylamine; 350 μmol) in NMP (1 mL) was incubated for 10 min for formation of the active ester. The reaction continued overnight with shaking at room temperature. The resin was then washed with DMF, treated with piperidine (20%) in DMF for 30 min, and washed again with DMF. Compounds **5** and **6** were synthesized as described previously.[5a] Compound **5** or **6** (175 μmol) was mixed with HBTU (61 mg, 160 μmol), HOBt (22 mg, 160 μmol), and DIPEA (350 μmol) in NMP (1 mL) and incubated for 10 min before being added to the resin. The acetyl protecting groups in **5** or **6** were removed by treatment with hydrazine (10%)/DMF for 5 h.[13] After being washed with DMF and THF, the resin was dried in vacuo. The dried resin was treated with cleavage cocktail (TFA/1,2-ethanedithiol/thioanisole = 95:2.5:2.5) for 3 h and then triturated with *tert*-butyl methyl ether. The triblock peptide was purified by RP HPLC (water/acetonitrile with 0.1% TFA). The molecular weight was confirmed by MALDI-TOF mass spectrometry (see Supporting Information).

TEM and CD Spectroscopy

For TEM, an aqueous solution of the sample (3 μL) was placed onto a holey carbon coated copper grid, and a solution of uranyl acetate (3 μL, 2% *w*/*w*) was added for negative staining. The sample was deposited for 1 min, and the excess solution was wicked off by filter paper. The dried specimen was observed with a JEOL-JEM 2010 instrument operating at 120 kV. The data were analyzed with DigitalMicrograph software. CD spectra were obtained on a JASCO model J-810 spectropolarimeter. Scans were performed in cuvettes of path length 0.1 cm and were repeated three times and averaged. The concentration was 25 μM. Molar ellipticity was calculated per amino acid residue.

E. coli Motility Inhibition and Agglutination Assay

An overnight culture of *E. coli* strain ORN178 was diluted to a concentration of 5×10^7 cells mL^{-1} with phosphate-buffered saline (PBS). The solution of *E. coli* (2 μL) was placed onto a glass slide, and serially diluted solutions (2 μL) of the nanoribbons in water were added. The sample was covered with a cover glass, and a layer of rubber cement was placed around the edges. The *E. coli* was observed with a Nikon Eclipse TE2000-U inverted fluorescence microscope equipped with a DXM1200C digital camera. For the motility-inhibition assay, the time-lapse images obtained were analyzed with Adobe Premiere software, and the ratio of nonmobile to mobile cells was calculated. The percentage motility inhibition was expressed as (number of nonmobile cells/number of total cells) × 100. The AI value was calculated from 10 random fields of microscopic images (920×690 μm^2), in which the number of cells in close contact were counted and averaged. For nile red fluorescence detection, a Y-2E/C filter set (Nikon, Japan) was used.

Encapsulation of Nile Red in the Nanoribbons

The dye nile red (60 ng, 0.2 nmol) was dissolved in acetonitrile (20 μL), and a solution of **3** (10 nmol) in water (20 μL) was added. The solution was sonicated, and PBS (40 μL) was slowly added. The sample was then lyophilized and redissolved in water.

Acknowledgements

We gratefully acknowledge the National Creative Research Initiative Program of the Korean Ministry of Science and Technology for financial support of this work.

[1] Reviews: a) J.-M. Lehn, *Proc. Natl. Acad. Sci. USA* **2002**, *99*, 4763–4768; b) L. Brunsveld, B. J. B. Folmer, E. W. Meijer, R. P. Sijbesma, *Chem. Rev.* **2001**, *101*,4071–4097; c) T. Shimizu, M. Masuda, H. Minamikawa, *Chem. Rev.* **2005**, *105*, 1401–1443; d) M. Lee, B.-k. Cho, W.-C. Zin. *Chem. Rev.* **2001**, *101*, 3869–3892; e) D. E. Discher, A. Eisenberg, *Science* **2002**, *297*, 967–973; f) J. A. A. W. Elemans, A. E. Rowan, R. J. M. Nolte, *J. Mater. Chem.* **2003**, *13*, 2661–2670; g) K. Kinbara, T. Aida, *Chem. Rev.* **2005**, *105*, 1377–1400; h) A. Mueller, D. F. O'Brien, *Chem. Rev.* **2002**, *102*, 727–757; i) D. Chen, M. Jiang, *Acc. Chem. Res.* **2005**, *38*, 494–502.

[2] A recent review: Y. b. Lim, M. Lee, *Org. Biomol. Chem.* **2007**, *5*, 401–405.

[3] a) M. Mammen, S. K. Choi, G. M. Whitesides, *Angew. Chem.* **1998**, *110*, 2908–2953; *Angew. Chem. Int. Ed.* **1998**, *37*, 2755–2794; b) C. R. Bertozzi, L. L. Kiessling, *Science* **2001**, *291*, 2357–2364; c) J. J. Lundquist, E. J. Toone, *Chem. Rev.* **2002**, *102*, 555–578; d) Y. C. Lee, R. T. Lee, *Acc. Chem. Res.* **1995**, *28*, 321–327; e) J. S. Kim, C. O. Pabo, *Proc. Natl. Acad. Sci. USA* **1998**, *95*, 2812–2817.

[4] a) B. S. Kim, D. J. Hong, J. Bae, M. Lee, *J. Am. Chem. Soc.* **2005**, *127*, 16333–16337; b) E. Fan, E. A. Merritt, C. L. M. J. Verlinde, W. G. J. Hol, *Curr. Opin. Struct. Biol.* **2000**, *10*, 680–686; c) P. I. Kitov, J. M. Sadowska, G. Mulvey, G. D. Armstrong, H. Ling, N. S. Pannu, R. J. Read, D. R. Bundle, *Nature* **2000**, *403*, 669–672; d) J. E. Kingery-Wood, K. W. Williams, G. B. Sigal, G. M. Whitesides, *J. Am. Chem. Soc.* **1992**, *114*, 7303–7305; e) J. Rojo, V. Diaz, J. M. de La Fuente, I. Segura, A. G. Barrientos, H. H. Riese, A. Bernad, S. Penades, *ChemBioChem* **2004**, *5*, 291–297;.

[5] a) Y.-b. Lim, S. Park, E. Lee, H. Jeong, J.-H. Ryu, M. S. Lee, M. Lee, *Biomacromolecules* **2007**, *8*, 1404–1408; b) J.-H. Ryu, E. Lee, Y.-b. Lim, M. Lee, *J. Am. Chem. Soc.* **2007**, *129*, 4808–4814; c) J. E. Gestwicki, L. E. Strong, C. W. Cairo, F. J. Boehm, L. L. Kiessling, *Chem. Biol.* **2002**, *9*, 163–169; d) M. D. Disney, J. Zheng, T. M. Swager, P. H. Seeberger, *J. Am. Chem. Soc.* **2004**, *126*, 13343–13346; e) A. B. Tuzikov, A. A. Chinarev, A. S. Gambaryan, V. A. Oleinikov, D. V. Klinov, N. B. Matsko, V. A. Kadykov, M. A. Ermishov, I. V. Demin, V. V. Demin, P. D. Rye, N. V. Bovin, *ChemBioChem* **2003**, *4*, 147–154; f) L. Gu, T. Elkin, X. Jiang, H. Li, Y. Lin, L. Qu, T.-R. J. Tzeng, R. Joseph, Y. P. Sun, *Chem. Commun.* **2005**, 874–876; g) H. Wang, L. Gu, Y. Lin, F. Lu, M. J. Meziani, P. G. Luo, W. Wang, L. Cao, Y.-P. Sun, *J. Am. Chem. Soc.* **2006**, *128*, 13364–13365.

[6] a) Y.-b. Lim, E. Lee, M. Lee, *Angew. Chem. Int. Ed.* **2007**, *46*, 3475–3478; b) H. Kodama, S. Matsumura, T. Yamashita, H. Mihara, *Chem. Commun.* **2004**, 2876–2877; c) A. J. Baldwin, R. Bader, J. Christodoulou, C. E. MacPhee, C. M. Dobson, P. D. Barker, *J. Am. Chem. Soc.* **2006**, *128*, 2162–2163; d) G. T. Dolphin, P. Dumy, J. Garcia, *Angew. Chem.* **2006**, *118*, 2765–2768; *Angew. Chem. Int. Ed.* **2006**, *45*, 2699–2702; e) C. W. G. Fishwick, A. J. Beevers, L. M. Carrick, C. D. Whitehouse, A. Aggeli, N. Boden, *Nano Lett.* **2003**, *3*, 1475–1479; f) D. M. Marini, W. Hwang, D. A. Lauffenburger, S. Zhang, R. D. Kamm, *Nano Lett.* **2002**, *2*, 295–299.

CHEMISTRY
AN ASIAN JOURNAL

[7] A. Aggeli, M. Bell, L. M. Carrick, C. W. Fishwick, R. Harding, P. J. Mawer, S. E. Radford, A. E. Strong, N. Boden, *J. Am. Chem. Soc.* **2003**, *125*, 9619–9628.
[8] a) T. S. Burkoth, T. L. S. Benzinger, D. N. M. Jones, K. Hallenga, S. C. Meredith, D. G. Lynn, *J. Am. Chem. Soc.* **1998**, *120*, 7655–7656; b) J. Hentschel, E. Krause, H. G. Börner, *J. Am. Chem. Soc.* **2006**, *128*, 7722–7723.
[9] a) K. Janek, J. Behlke, J. Zipper, H. Fabian, Y. Georgalis, M. Beyermann, M. Bienert, E. Krause, *Biochemistry* **1999**, *38*, 8246–8252; b) C. L. Nesloney, J. W. Kelly, *Bioorg. Med. Chem.* **1996**, *4*, 739–766.
[10] S. L. Harris, P. A. Spears, E. A. Havell, T. S. Hamrick, J. R. Horton, P. E. Orndorff, *J. Bacteriol.* **2001**, *183*, 4099–4102.
[11] a) L. S. L. Yu, S. A. Reed, M. H. Golden, *J. Microbiol. Methods* **2002**, *49*, 63–68; b) H. Stender, K. Oliveira, S. Rigby, F. Bargoot, J. Coull, *J. Microbiol. Methods* **2001**, *45*, 31–39.
[12] a) J. J. Martinez, M. A. Mulvey, J. D. Schilling, J. S. Pinkner, S. J. Hultgren, *EMBO J.* **2000**, *19*, 2803–2812; b) M. A. Mulvey, Y. S. Lopez-Boado, C. L. Wilson, R. Roth, W. C. Parks, J. Heuser, S. J. Hultgren, *Science* **1998**, *282*, 1494–1497; c) D. Mirelman, G. Altmann, Y. Eshdat, *J Clin Microbiol* **1980**, *11*, 328–331.
[13] P. Virta, M. Karskela, H. Lönnberg, *J. Org. Chem.* **2006**, *71*, 1989–1999.

Received: May 8, 2007
Revised: June 11, 2007
Published online: September 11, 2007

